Electronic Supplementary Material (ESI) for New Journal of Chemistry.

Evaluating an effective Electrocatalyst for the rapid determination of Triptan drug (MaxaltTM) from (Mono and Binary) Transition Metal (Co, Mn, CoMn, MnCo) Oxides via. Electrochemical approaches

S1. *Materials and instrumentations*

Ethanol and sodium hydroxide were purchased from Sigma-Aldrich (http://www.sigmaaldrich.com/taiwan.html) and utilized without any purifications. The supporting electrolyte consumed for the electrochemical studies is 0.1 M phosphate buffer pH 7. The resulting plots exhibited were the average of no less than three experiments. The error bars were provided from the standard deviation of those three measurements.

The electrochemical experiments were carried out through CHI 1205A workstation. The experiments were done in a conventional three-electrode cell using glassy carbon electrode as a working electrode (area 0.07 cm^2), Pt wire as a counter electrode, and saturated Ag/AgCl as a reference electrode. DPV curves were obtained through the CHI 900 as a working station. The X-ray photoelectron spectroscopy studies were done through a PerkinElmer PHI-5702. Field Emission Scanning electron microscopy (FE-SEM) studies were made with Hitachi S-3000 H scanning electron microscope. Powder X-ray diffraction (PXRD) studies were completed in an XPERT-PRO (PANalytical B.V., The Netherlands) diffractometer using Cu Kα radiation (k=1.54 Å).

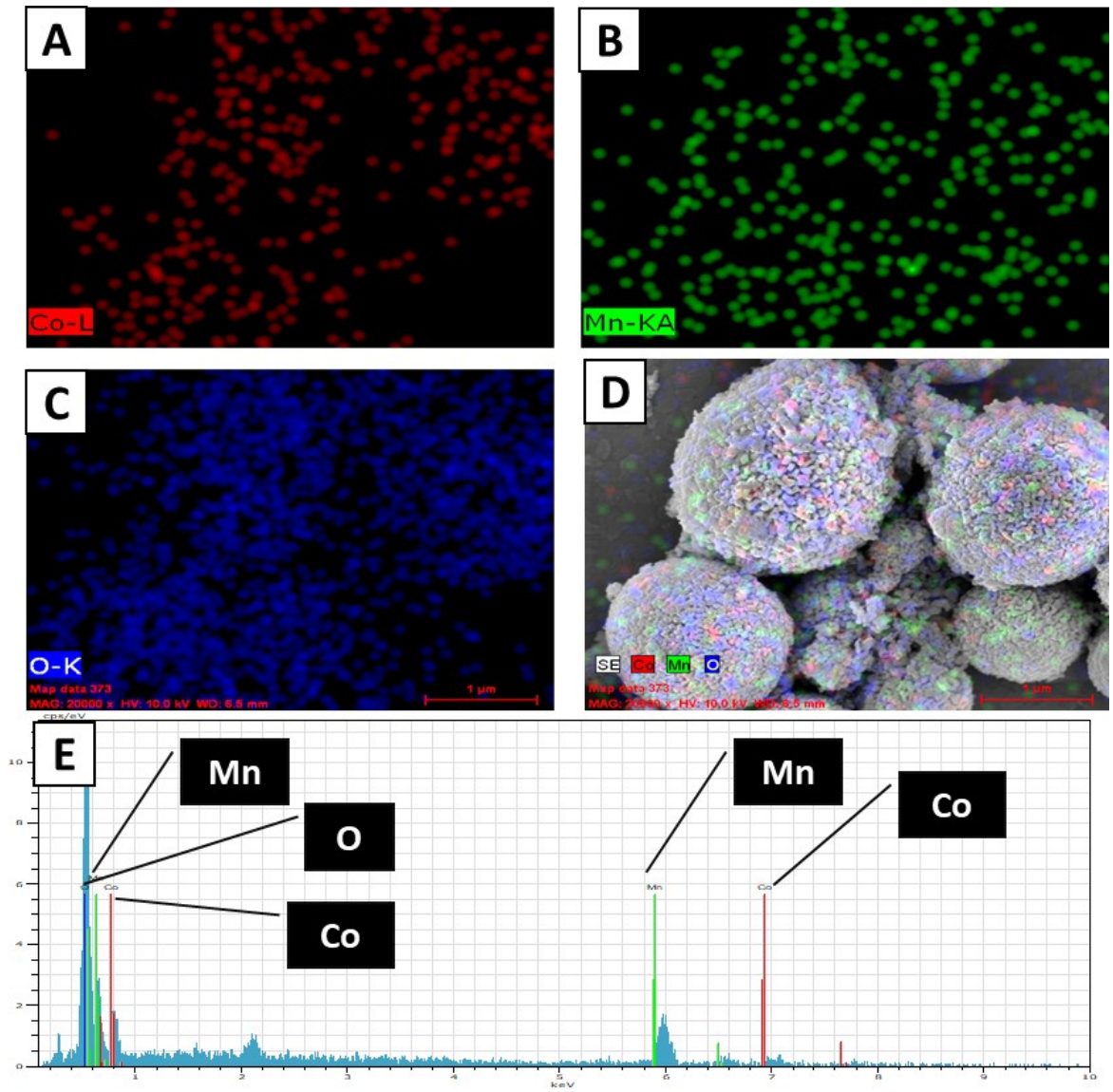

Fig. S1. Mapping (A-D) and EDX profile (E) of $CoMn_2O_4$ HMs

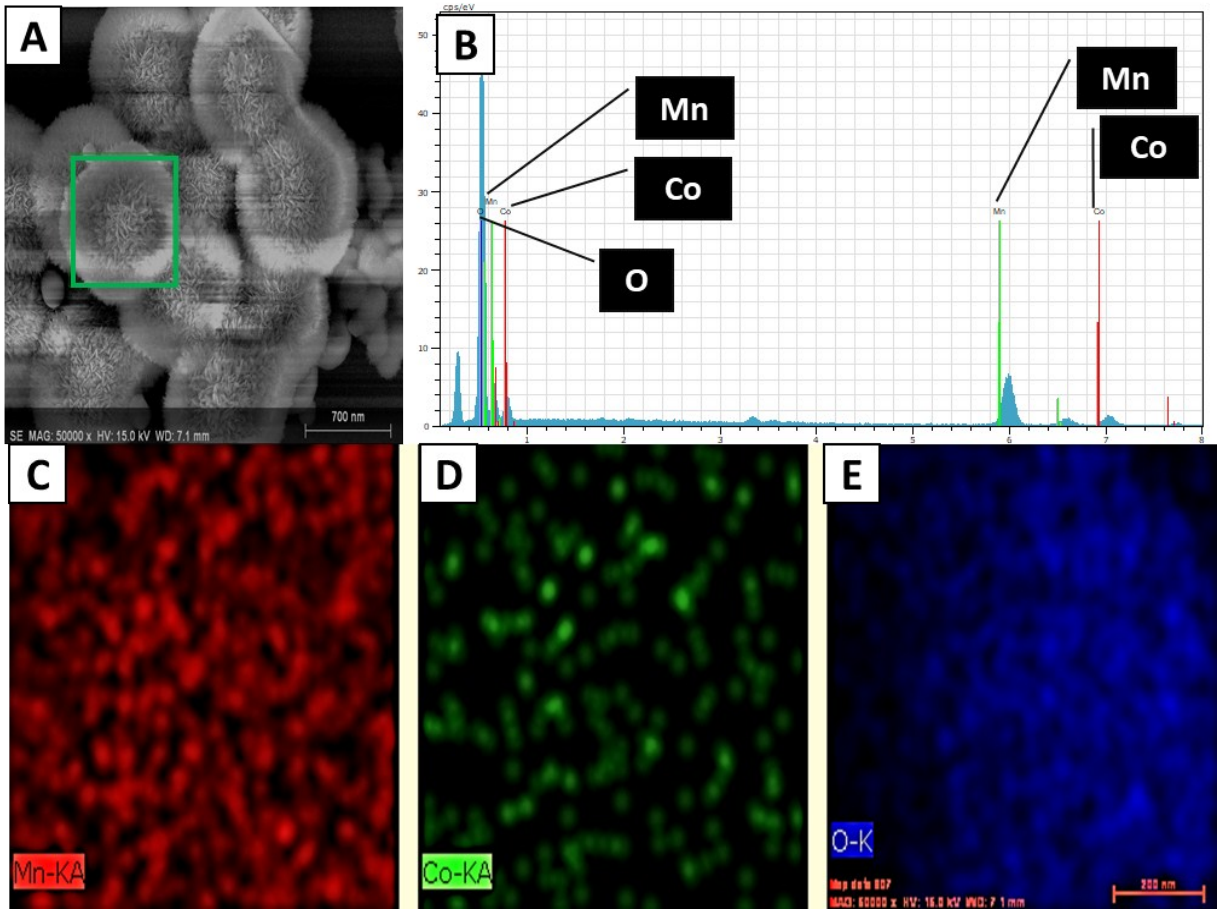

Fig. S2. Corresponding SEM image (A), EDX profile (B) and Mapping (C-E) of $MnCo_2O_4$ MFs

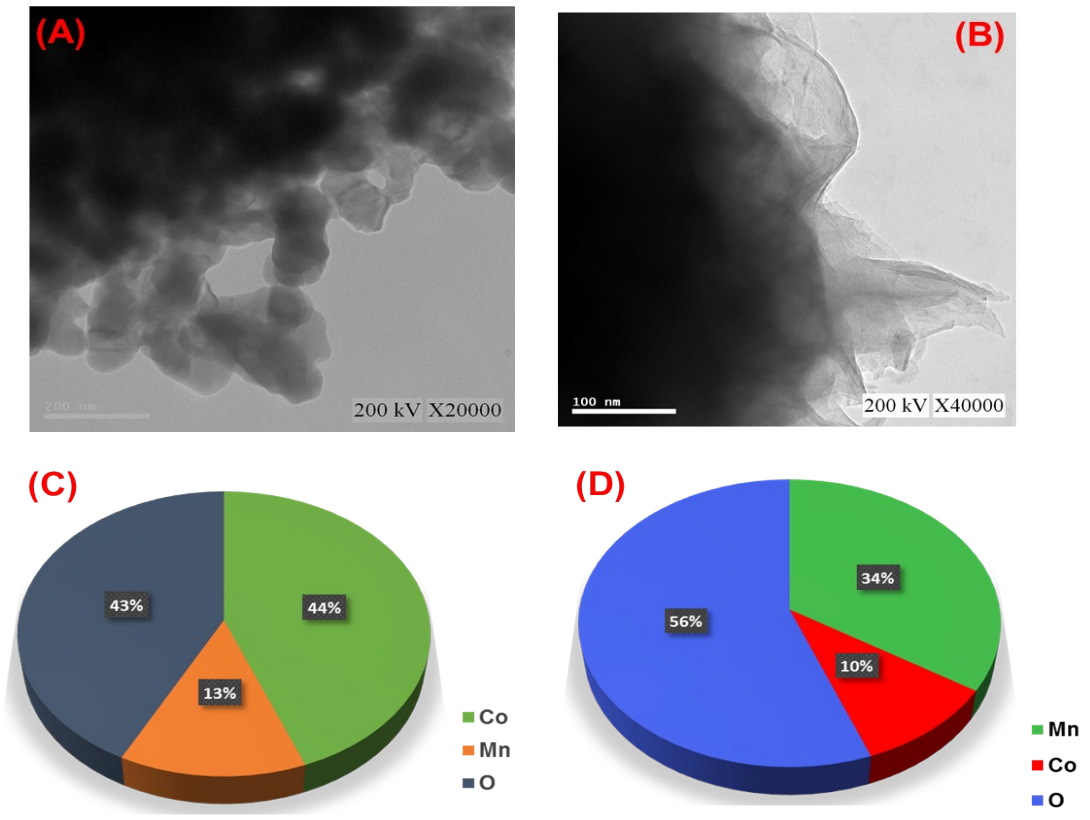

Fig. S3. HR-TEM on the edge of $CoMn_2O_4$ HMs (A) and $MnCo_2O_4$ MFs (B). The weight perctange of $CoMn_2O_4$ HMs (C) and $MnCo_2O_4$ MFs (D)

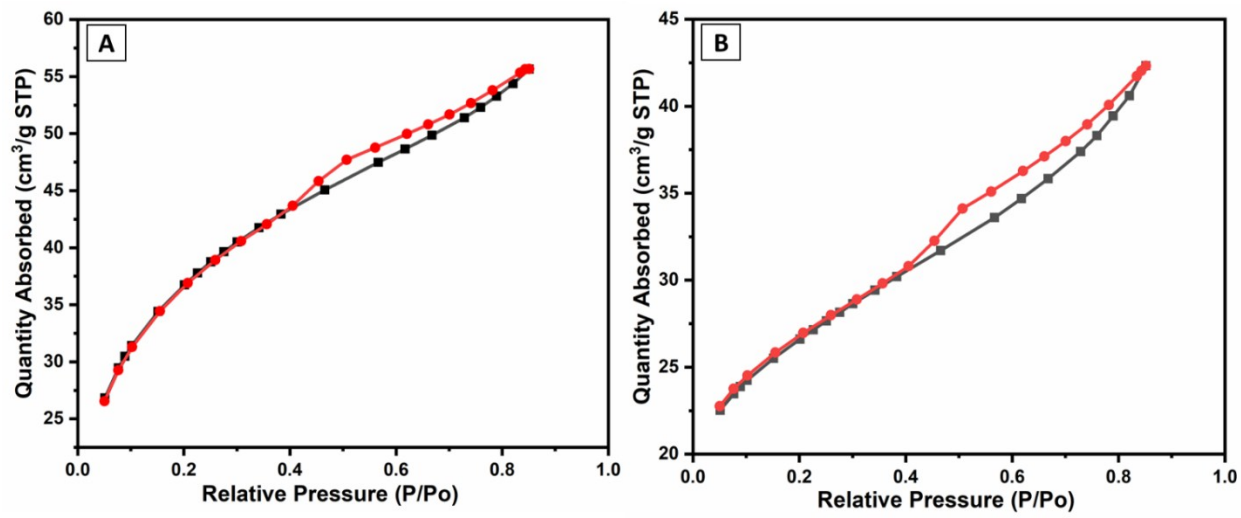

Fig. S4. BET isotherms of $CoMn_2O_4$ HMs (A), and $MnCo_2O_4$ MFs (B). (Black line: Adsorption, and Redline: Desorption)

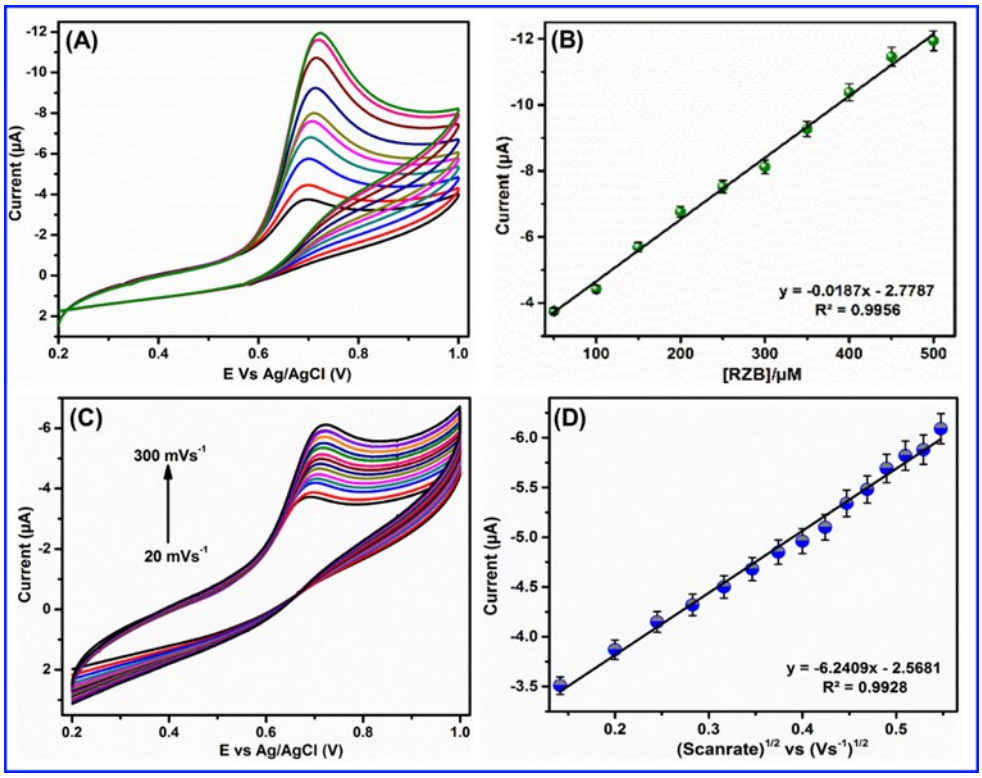

Fig. S5. (A) CVs of $CoMn_2O_4$ HMs/GCE containing a various concentration of RZB (50 to 500μM) in pH-7. (B) Calibration plot [RZB/μM] vs. peak currents (μA). (C) CVs of $CoMn_2O_4$ HMs /GCE at different scan rates of (20 to 300 mVs^{-1}) in 0.1M pH-7 containing 100 μM of RZB. (D) Corresponding calibration plot of the square root of scan rates versus oxidation peak current (μA).

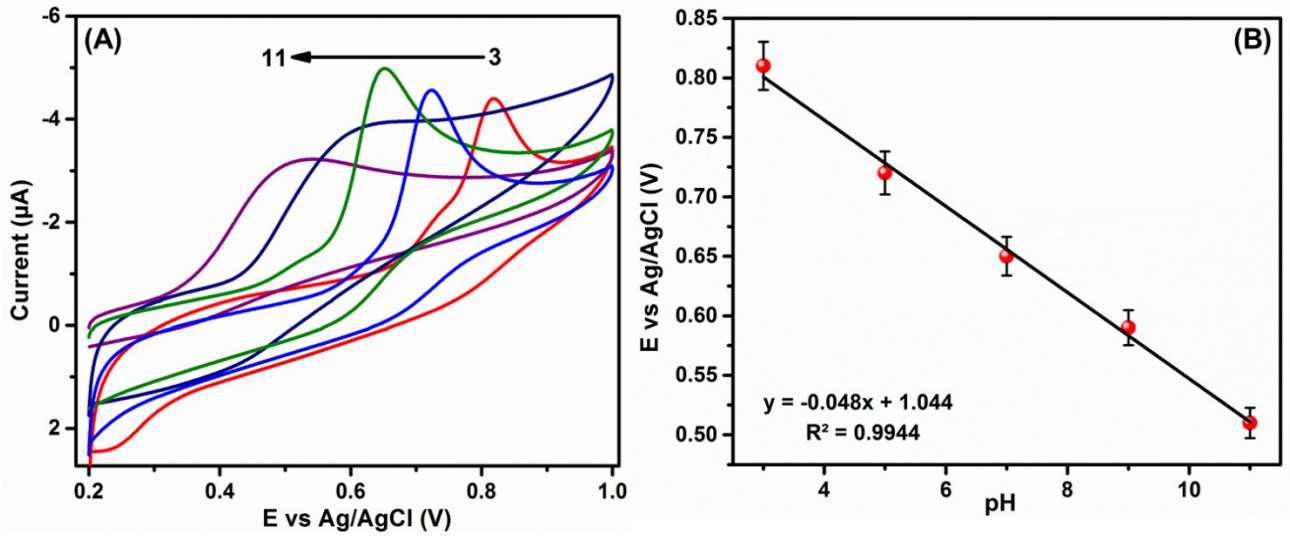

Figure S6. (A) CV's of different pH ranges from (3-11). (B) Linear calibration plot of pH versus peak potential.

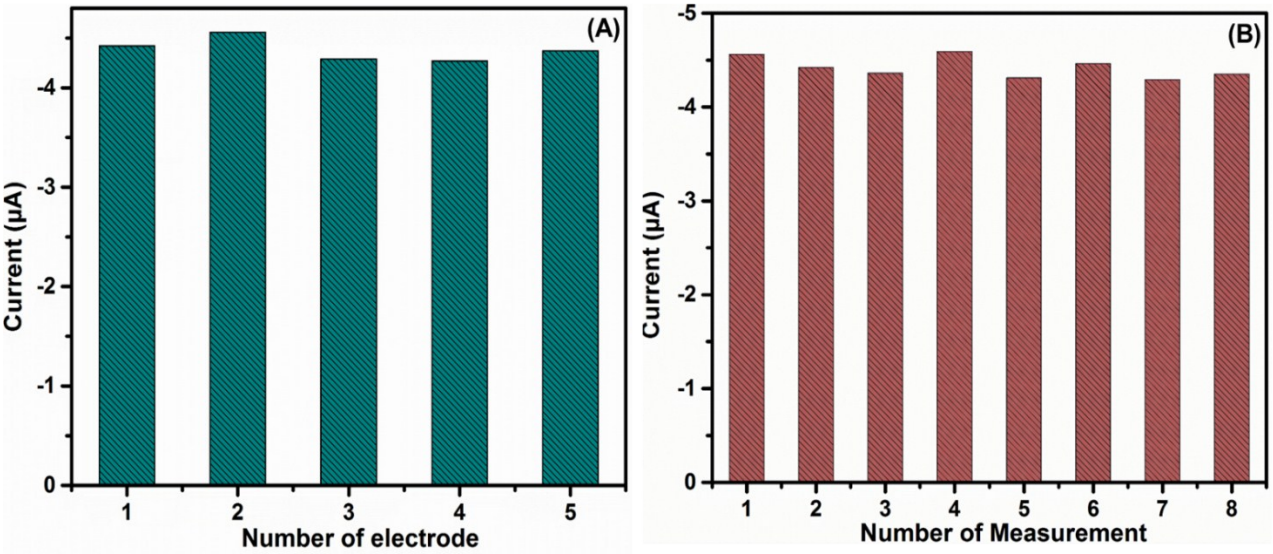

Figure S7. (A) Plot for the repeatability of the developed sensor. (B) Reproducibility plot of $CoMn_2O_4$ MHs/GCE towards the detection of RZB.

Table S1. Comparing the determination of RZB in oral tablets and human serum samples by the developed sensor

S.NO	Real sample	Added (μM)	Found(μM)	Recovery (%)	RSD (%)
1.	Tablets	2	2.09 (±0.09)	104.5	3.69
		5	4.99 (±0.12)	99.8	3.01
2.	Human serum	2	1.91 (±0.2)	95.5	2.27
		5	4.84 (±0.18)	96.8	3.41

[a]R.S.D- Relative standard deviation